J Sol-Gel Sci Technol (2009) 49:137–144
DOI 10.1007/s10971-008-1870-5

FAST TRACK COMMUNICATION

CAM sol–gel synthesized $LiMPO_4$ (M=Co, Ni) cathodes for rechargeable lithium batteries

Gangulibabu · D. Bhuvaneswari · N. Kalaiselvi · N. Jayaprakash · P. Periasamy

Received: 9 September 2008 / Accepted: 25 November 2008 / Published online: 10 December 2008

Abstract The emerging category cathode candidates such as $LiCoPO_4$ and $LiNiPO_4$ were synthesized at 800 °C using Citric acid assisted modified sol–gel (CAM sol–gel) method and examined for possible lithium intercalation behavior. Compound formation temperature is confirmed from thermogravimetry and differential thermal analysis (TG/DTA). Powder X-ray diffraction (PXRD) pattern evidenced the absence of undesirable peaks and confirmed the formation of phase pure $LiMPO_4$ (M=Co, Ni) compounds with an orthorhombic structure and finer crystallite size. Presence of nanosized particles as observed from TEM image of $LiCoPO_4$ and the presence of preferred local cation environment as understood from FT–IR studies are the added advantages of CAM sol–gel synthesis. Further, Cyclic voltametry (CV) and Impedance spectroscopy (EIS) studies performed on the synthesized $LiCoPO_4$ and $LiNiPO_4$ cathodes revealed excellent reversibility and structural stability of CAM sol–gel synthesized cathodes, especially upon storage as well as during cycling.

Gangulibabu · D. Bhuvaneswari · N. Kalaiselvi (✉) · N. Jayaprakash · P. Periasamy
Central Electrochemical Research Institute, 630 006 Karaikudi, Tamilnadu, India
e-mail: kalakanth2@yahoo.com

Gangulibabu
e-mail: gangula.babu@yahoo.com

D. Bhuvaneswari
e-mail: bhuvanarajj@gmail.com

N. Jayaprakash
e-mail: reddyic2002@yahoo.co.in

P. Periasamy
e-mail: psamy31@rediffmail.com

Keywords CAM sol–gel method · $LiCoPO_4$ · $LiNiPO_4$ · XRD · Cyclic reversibility

1 Introduction

Rechargeable lithium batteries which are commonly used in consumer electronics possess salient features such as high energy density, less weight, no memory effect, negligible self discharge, etc., due to which the same are popular in defense, automotive, and aerospace applications. Among the various components of lithium-ion batteries, certain cathodes viz., $LiMO_2$ layered oxide such as cobalt oxide or nickel oxide, spinel oxide such $LiMn_2O_4$ type and a $LiMPO_4$ type olivine such as lithium iron phosphate have been accepted as potential cathode candidates. Hereagain, layered $LiCoO_2$, though known as a successful commercial material in small size batteries, suffers from lack of safety upon overcharge [1] and the possibility of realizing lower deliverable capacity compared to higher theoretical capacity. $LiNiO_2$ on the other hand is limited by its lower thermal stability, off-stoichiometry problem, and the requirement of stringent synthesis conditions. Similarly, the spinel $LiMn_2O_4$ has no degree of freedom for opening the interstitial space of the close packed oxide-ion array in which the Li^+ ions generally move [2] and suffers from John-Teller distortion also, due to known reasons.

Regarding phosphate olivines, research is focused on the $LiFePO_4$ cathode in the recent years, due to its inherent advantages such as safety, economic viability, eco benign nature, and abundant availability. But the poor electronic conductivity and stringent synthesis methodology of $LiFePO_4$ are the major hampering issues against the commercialization of the same [3, 4]. To address the same, several attempts are being reported on the reduction of

particle size [5], carbon nanopainting, otherwise known as coating or co-synthesizing of compounds with carbon [6–8], doping of supervalent metal cations [9], etc., in order to improve the electrochemical properties of native $LiFePO_4$. However, the synthesis of $LiFePO_4$ despite having reached the commercial status, still poses issues on the amount, type, and the mode of carbon addition to realize LiFePO4 with appreciable energy as well as power density required for the heavy electrical vehicles (HEV) applications. As a result, research on other possible olivine cathodes with transition metals like Co or Ni to form $LiCoPO_4$ and $LiNiPO_4$, respectively, has gaining importance. Towards this direction, the present work is planned on the synthesis and characterization of $LiCoPO_4$ and $LiNiPO_4$ cathodes, especially through the less studied solution assisted method, namely citric acid assisted modified sol gel (CAM sol–gel) method.

It is well-known that the rate capability of lithium-ion batteries could be enhanced by way of reducing the particle size of electrode materials [10]. Also, it is well reported that the synthesis procedure plays a vital role in reducing the particle size and the related improvement in terms of physical as well as electrochemical properties of synthesized cathode materials [11]. Hence, CAM sol–gel method exploited so far against the synthesis of oxide cathode materials and known for producing meso structured compounds has been chosen for present study to synthesize newer category LiMPO4 (M=Co, Ni) compounds [12].

Herein, the currently adopted CAM sol–gel method, based on solution approach ensures the uniform distribution and an atomic level mixing of reactants and gelling agents. Such an intimate mixing of precursors render phase pure final products with nanoparticle size, which is the significance of CAM sol–gel method. In this method, both the acrylamide and N′,N-methylene-bis-acrylamide act as gelling agents, whereas citric acid with a molecular formula of $C_6H_8O_7 \cdot H_2O$ acts as a fuel for the formation of bond between the transition metal ions and phosphate polyanion as described schematically in Fig. 1. Originally, the carboxylic acid group that is present in the complexing agent citric acid forms a chemical bond with the metal ions, which upon evaporation of solvent leads to the formation of viscous gel like paste precursor. It is presumed that the metal ions are trapped inside the so called viscous gel to ensure atomic level mixing, which is the key point of the CAM sol–gel method.

Hence, CAM sol–gel synthesized cathode candidates are expected to exhibit enhanced battery performance, due to much shorter diffusion distances of the intercalating Li^+ ions. Interestingly, CAM sol–gel method of the present study has resulted in the formation of nanosized $LiCoPO_4$ and $LiNiPO_4$ powders with desirable physical and electrochemical characteristics, which is in accordance with the focal theme of the present work.

2 Experimental details

2.1 Synthesis procedure

$LiCoPO_4$ and $LiNiPO_4$ cathode powders were synthesized from stoichiometric ratios of the starting materials viz., $LiOOCCH_3 \cdot 2H_2O$ (Lithium acetate, Merck), $(CH_3COO)_2Co \cdot 4H_2O$/$(CH_3COO)_2Ni \cdot 4H_2O$ (Cobalt acetate/Nickel acetate, Merck) and $NH_4H_2PO_4$ (Ammonium dihydrogen phosphate, Merck). Primarily, the reactants were dissolved in hot water with stirring to get a homogeneous solution. To the solution, calculated amount of citric acid, acryl amide, and finally N,N′-methylene-bis-acrylamide were added and the process of stirring and heating were continued. At this point, it is quite interesting to note that as soon as the N,N′-methylene-bis-acrylamide was added, the viscosity of the homogeneous solution increased drastically and the same upon further heating and stirring has formed a transparent gel. Further, it is understood that citric acid acts as not only as a chelating agent but also as a fuel to reduce the heat energy supplied and the added acryl amide acts as a buffering agent to adjust the pH required for the transparent gel formation. Similarly, the added N,N′-methylene-bis-acrylamide facilitates the rapid formation of transparent gel, via. formation of meta stable chelated complex. Representative schematic diagram with a mechanism involved in the synthesis of $LiMPO_4$ (M=Co, Ni) using CAM sol–gel method is displayed in Fig. 1.

The thus formed gels were dried at 110 °C for about 12 h in a hot air oven initially and the dried samples were further ground and furnace-heated to 300 °C for about 6 h The resultant powders were also ground again and fired further at 800 °C for about 5 h using alumina crucibles. Herein, both the rate of heating and cooling in the furnace heating were maintained at 10 °C/min to avoid surface cracking of the particles and to ensure the presence of uniformly distributed particles of nanosize. The ultrafine powders of $LiCoPO_4$ and $LiNiPO_4$ obtained after 800 °C were collected and subjected to systematic physical as well as electrochemical characterizations.

2.2 Physical and electrochemical characterizations

Compound formation temperature was confirmed by thermogravimetry and differential thermal analysis (TG/DTA) with a thermo balance model STA 409 PC in the temperature range 25–800 °C, using alumina crucibles, under air with a heating rate of 20 °C/min. Phase characterization was done by powder X-ray diffraction technique on a Philips 1830 X-ray diffractometer using Ni-filtered Cu$K\alpha$ radiation ($\lambda = 1.5406$A°) in the 2θ range 10–90° at a scan rate of 0.04°/s. Fourier transform infrared spectroscopic (FT–IR) study was performed on a Perkin–Elmer paragon

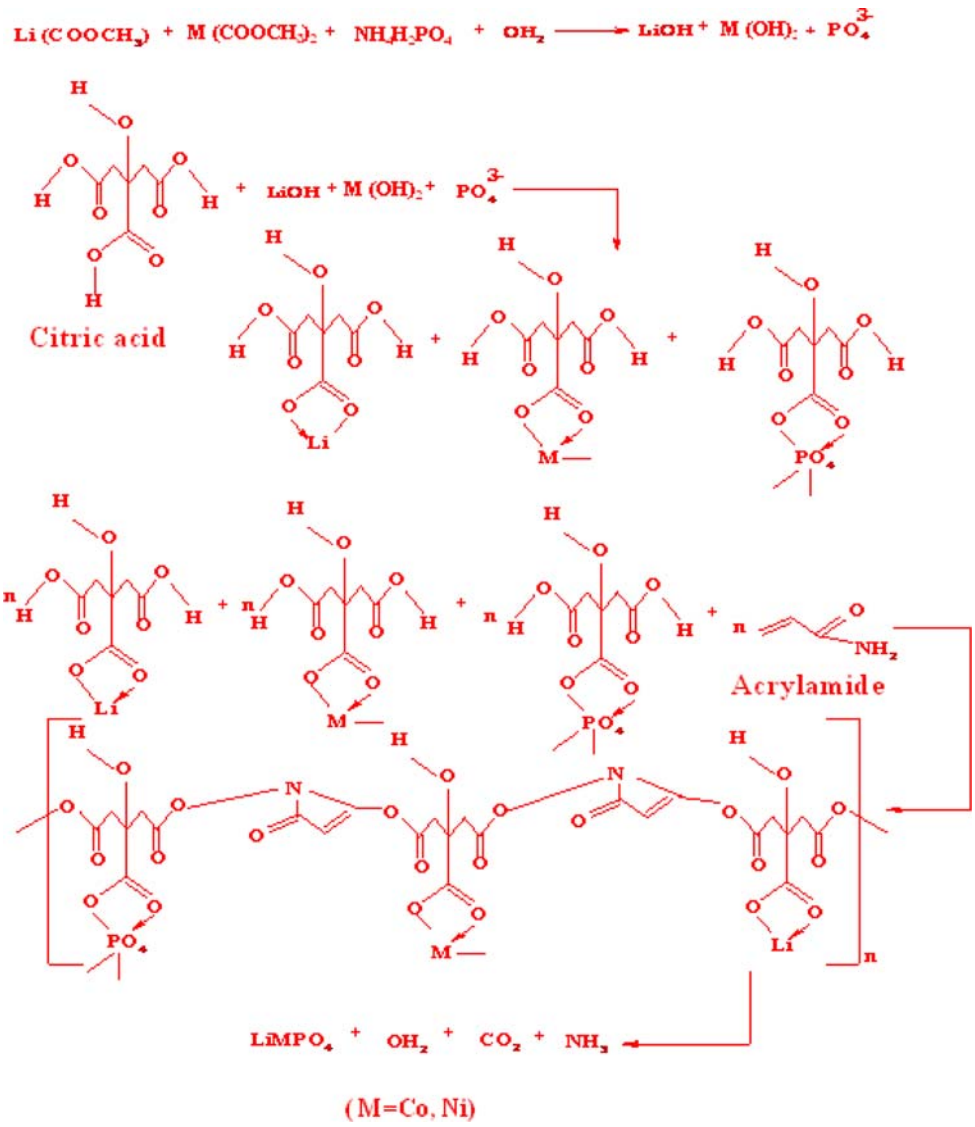

Fig. 1 Chemical reaction mechanism involved in the CAM sol–gel method to synthesize $LiMPO_4$ (M=Co, Ni) compounds

−500 FTIR spectrophotometer using a pellet containing a mixture of KBr and the active materials in the region 400–2,000 cm^{-1}. Electron paramagnetic resonance (EPR) measurements were carried out using a Bruker instrument. Room temperature electrochemical studies such as cyclic voltametry (CV) and Electrochemical Impedance Spectroscopy (EIS) measurements were performed using an Auto lab electrochemical workstation, wherein CV scan rate was fixed as 1 mV/s and impedance analysis was done over a frequency range of 100 KHz–0.1 Hz.

2.3 Electrode preparation and coin cell fabrication

To prepare cathode electrode, the synthesized powder was first mixed intimately with super P carbon black (additive) and polyvinylidene fluoride (binder) in 80:10:10 ratio, respectively, and the same was treated with *N*-Methylpyrrolidin-2-one (solvent) to form a slurry. The slurry was cast uniformly on a thin aluminum foil (20 μm) and then dried for about 2 h at 110 °C. The dried foil was hot pressed (under 5 ton pressure) and the circular electrodes were punched out from the coated foil. Using such cathodes, 2016 coin cells were assembled in an Argon-filled glove box and crimp sealed prior to electrochemical studies. CV and EIS characterizations were carried out on such type of 2016 coin cells consisting of lithium anode, synthesized $LiMPO_4$ (M=Co, Ni) cathode and a non-aqueous electrolyte containing 1 M $LiPF_6$ dissolved in 1:1 v/v EC:PC with a cell guard separator.

3 Results and discussion

3.1 Thermal analysis

Figures 2a and b show the thermogravimetric and differential thermal analysis (TG/DTA) scans of the mixtures

containing the fine ground precursors of $LiCoPO_4$ and $LiNiPO_4$, respectively. In the case of $LiCoPO_4$, TG curve shows a gradual and an initial weight loss up to about 450 °C due to the initial evaporation of water (below 200 °C) and a subsequent decomposition of precursors (200–450 °C) from the in-situ formed meta stable complex. In other words, the decomposition of citric acid and amides to release CO_2 and NH_3 followed by the final decomposition of chelated metal acetate are obvious from the larger exothermic peak observed at 440 °C in the DTA curve. Herein, the compound formation process starts at a temperature as low as 325 °C and the same gets completed around 570 °C only. Since no significant weight loss has been observed especially beyond 570 °C, it is deduced that the compound formation process gets completed well within 570 °C itself. Such a thermal stability of $LiCoPO_4$ beyond 600 °C has already been reported by Chen et al. [13] and the current observations related to the TG/DTA behavior of chosen category precursors of $LiCoPO_4$ are also in good agreement with the same. Hence, it is confirmed from this study that the complete compound formation of $LiCoPO_4$ is taking place well below 600 °C itself. However, the sample of the present study was heat treated further to 800 °C in order to get phase pure and better crystalline product.

Figure 2b shows that the precursors of $LiNiPO_4$ also exhibits a continuous weight loss up to 550 °C due to the evaporation of water and the decomposition aided evaporation of gases like CO_2 and NH_3, as in the case of $LiCoPO_4$. Similarly, it is obvious from Fig. 2b that the compound formation process starts at 350 °C and gets completed at 550 °C. After 550 °C, negligible weight loss in TG curve has been observed which confirms the complete formation of phase pure $LiNiPO_4$ compound at 550 °C itself. Despite the same, as in the previous case, the powder of $LiNiPO_4$ has also been heat treated further at 800 °C for about 5 h, for reasons of realizing better purity and crystallinity.

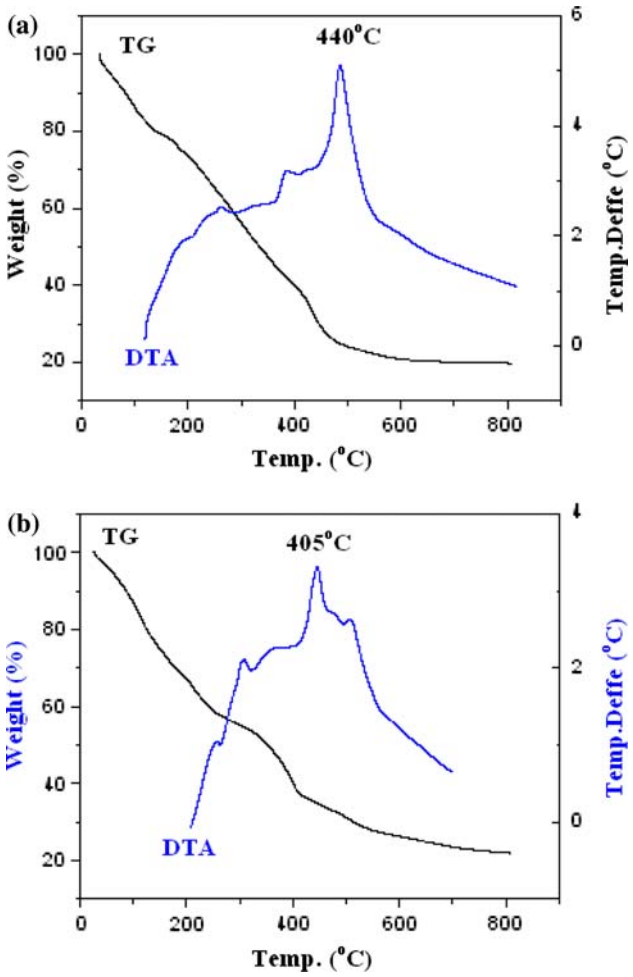

Fig. 2 **a** TG/DTA behavior of $LiCoPO_4$ and **b** TG/DTA behavior of $LiNiPO_4$

3.2 Phase characterization

The XRD patterns of $LiCoPO_4$ and $LiNiPO_4$ compounds synthesized by CAM sol–gel method are shown in Figs. 3a and b, respectively. The existence of well defined and highly intense peaks with the absence of unknown Bragg peaks confirms the presence of crystalline and phase pure products of desired category. The miller indices (hkl) of all the peaks corresponding to those of $LiCoPO_4$ and $LiNiPO_4$ are indexed as per the JCPDS file numbers 89–6192 and 88–1297, respectively. From search match analysis, it is deduced that both the compounds possess orthorhombic structure with Pnma space group. Further, lattice parameter (a, b, c) values were calculated using iterative least square analysis and the corresponding cell volume values have also been calculated for $LiCoPO_4$ and $LiNiPO_4$ individually (Table 1).

Similarly, the average crystallite size (D) has been calculated using Scherer's formula [14], which is in favor of significantly reduced nanometric crystallite size of $LiCoPO_4$ and $LiNiPO_4$ (<50 nm). Herein, it is believed that the presence of nanometric crystallites of $LiCoPO_4$ and $LiNiPO_4$ are due to the impact of the CAM sol–gel method. In addition, Table 1 infers that the calculated stoke's strain values are also found to be very small, which is an indication for the presence of strain free crystal lattice in the CAM sol–gel synthesized phosphate olivines. As, it is deduced qualitatively from XRD (using Scherrer's formula) that the olivines synthesized using CAM sol–gel method are found to possess nanometric crystallite size, the same has been intended to verify from TEM studies also.

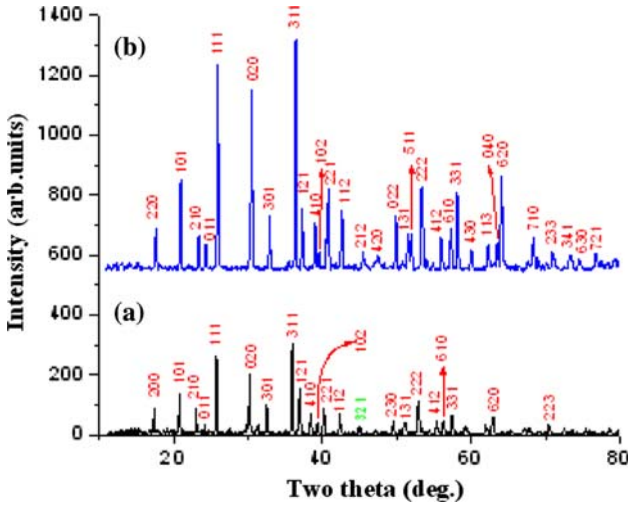

Fig. 3 PXRD pattern of (**a**) $LiCoPO_4$ and (**b**) $LiNiPO_4$ synthesized by CAM sol–gel method

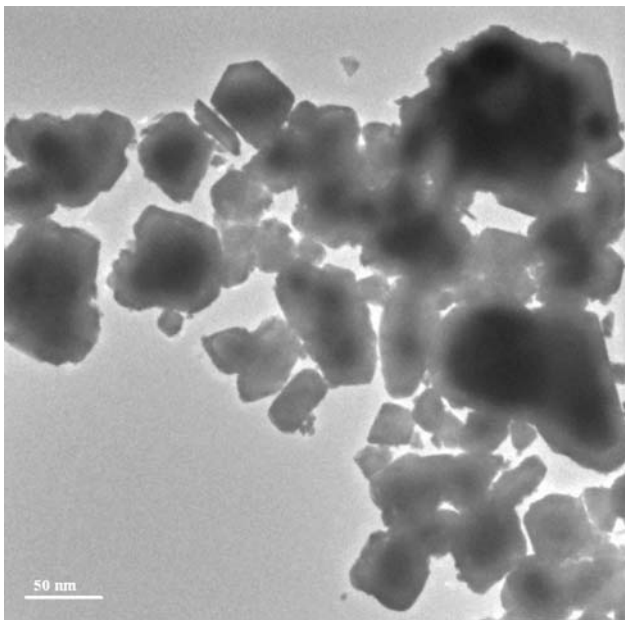

Fig. 4 TEM image of $LiCoPO_4$ synthesized by CAM sol–gel method

3.3 Transmittance electron microscope (TEM) study

In order to examine the actual size of the particles produced by CAM sol–gel method, TEM image was recorded for $LiCoPO_4$ and the result is displayed in Fig. 4. Interestingly, TEM picture of $LiCoPO_4$ exhibits the presence of 50 nm particles, thus substantiating the qualitative results derived from XRD. Hence, it is confirmed from TEM studies also that CAM sol–gel method is effective in reducing the size of the particles significantly, which is desirable for lithium inserting cathode materials.

3.4 Local cation environment by FTIR

Generally, Fourier transform infrared (FTIR) spectroscopy is sensitive to the short range environment of oxygen coordination around the cation in an oxide lattice. With regard to the factor group analysis and molecular vibration model [15] suggested to understand the structure of phospho-olivines, it is obvious from the current study also that the fundamental frequencies of PO_4^{3-} polyanions are split in to many components (v_1–v_4) due to the correlation effect which in turn is induced by the coupling of M–O bonds. As a result, the vibration spectra of $LiCoPO_4$ and $LiNiPO_4$ are dominated by the fundamental vibrations of PO_4^{3-} polyanions, which is not unusual [15]. Figure 5a shows four fundamental vibrations of PO_4^{3-} such as an asymmetric stretching mode at v_1–971 cm^{-1}, a doublet at around v–472 cm^{-1} and two triplets viz., v_3 and v_4 in the region 1,055–1,106 cm^{-1} and at 646 cm^{-1}. Further, the observed peaks at 509 cm^{-1} and 581 cm^{-1} region are attributed to the asymmetric stretching modes of CoO_6 octahedra [16], thus confirming the presence of $LiCoPO_4$.

In the case of $LiNiPO_4$ (Fig. 5b), the fundamental vibrations include an asymmetric stretching mode at v–965 cm^{-1}, a doublet around v–472 cm^{-1} and two triplets v_3 and v_4 in the regions 1,051–1,109 cm^{-1} and 582–653 cm^{-1}. Besides the fundamental vibrations of PO_4^{3-} polyanions, the peak observed around 545 cm^{-1} may be ascribed to the asymmetric stretching of Ni–O bonds in NiO_6 octahedra [17] and the other peak at 408 cm^{-1} may be attributed to the bending modes of O–Ni–O bonds. Hence, the structure of $LiNiPO_4$ could be understood.

Basically v_1 and v_3 modes involve the symmetric and antisymmetric stretching vibration of the P–O bonds, where as v_2 and v_4 modes involve mainly O–P–O symmetric and antisymmetric bending modes with a small contribution of P vibration [18]. Also the FTIR spectra obtained in the present study are comparable with those of the results obtained in same of the earlier studies on phosphate based compounds [19], thus confirming the fact that all the PO_4^{3-} tetrahedra possess stable chemical bonds

Table 1 Physical parameters of $LiCoPO_4$ and $LiNiPO_4$ compounds

Compound	Lattice constants (A°)			Cell volume (A^{o3})	Avg. crystallite size (nm)	Stoke strain
	a	b	c			
$LiCoPO_4$	10.2	5.91	4.73	285.13	48.9	2.5×10^{-3}
$LiNiPO_4$	10.03	5.85	4.69	275.19	40.6	3.1×10^{-3}

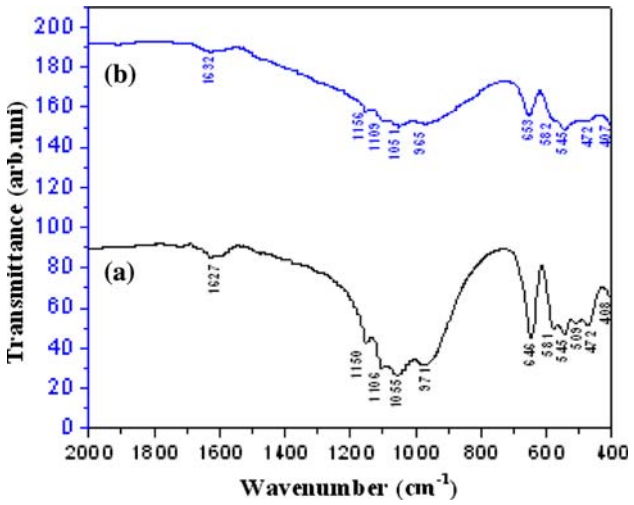

Fig. 5 FTIR Spectra of (**a**) $LiCoPO_4$ and (**b**) $LiNiPO_4$

and thereby producing $LiCoPO_4$ and $LiNiPO_4$ compounds with preferred local cation environment.

3.5 Room temperature EPR studies

In order to understand the possible existence of difference in electronic structure and the related magnetic properties of $LiMPO_4$ (M=Co, Ni) cathodes [20], EPR study was carried out for $LiCoPO_4$ and $LiNiPO_4$ individually and the results of the same are displayed in Fig. 6. Herein, the frequency of the microwave field is 9.9778 GHz and the frequency of the ac modulation magnetic field is 100 kHz. Under such conditions, the EPR signals are found to get centered at 3275G (g−2.16) and 3384G (g−2.06) for $LiCoPO_4$ and $LiNiPO_4$, respectively. $LiCoPO_4$ shows a broad signal that may be attributed to the insufficient electronic spin density for the transition to take place at room temperature. But $LiNiPO_4$ shows a finer signal along with a hyperfine splitting due to the interaction of unpaired electron with the neighboring nuclei. Thus, the presence of low-spin Ni^{2+} and high-spin Co^{2+} pertinent to $LiNiPO_4$ and $LiCoPO_4$ compounds could be understood.

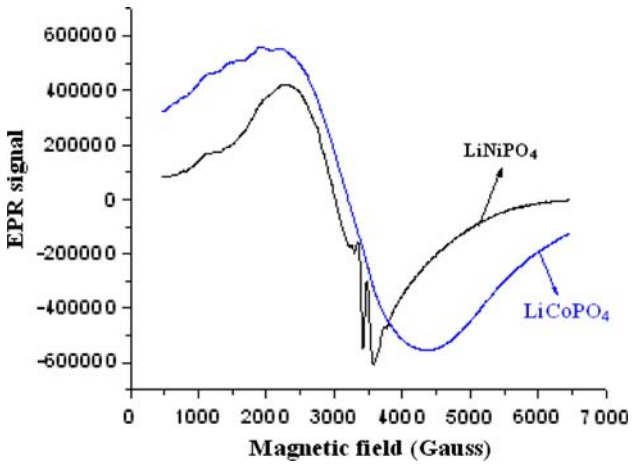

Fig. 6 EPR spectrums of $LiCoPO_4$ and $LiNiPO_4$

3.6 Electrochemical properties

3.6.1 Cyclic voltametry studies

Figures 7a and b show the representative cyclic voltamograms of $LiCoPO_4$ and $LiNiPO_4$ compounds, recorded at room temperature with the scan rate of 1 mV/sec *vs* Li/Li^+. Figure 7a shows two representative cyclic voltamograms recorded in the potential range 2.5–4.8 V and 2.5–5.2 V individually. It is interesting to note that when $LiCoPO_4$ is cycled between 2.5 and 4.8 V, the presence of prominent anodic peak (de-intercalation) at 3.8 V and a corresponding cathodic peak (intercalation) at 3.3 V are seen. On the other hand, when $LiCoPO_4$ cathode is cycled in the extended potential range of 2.5–5.2 V, a predominant

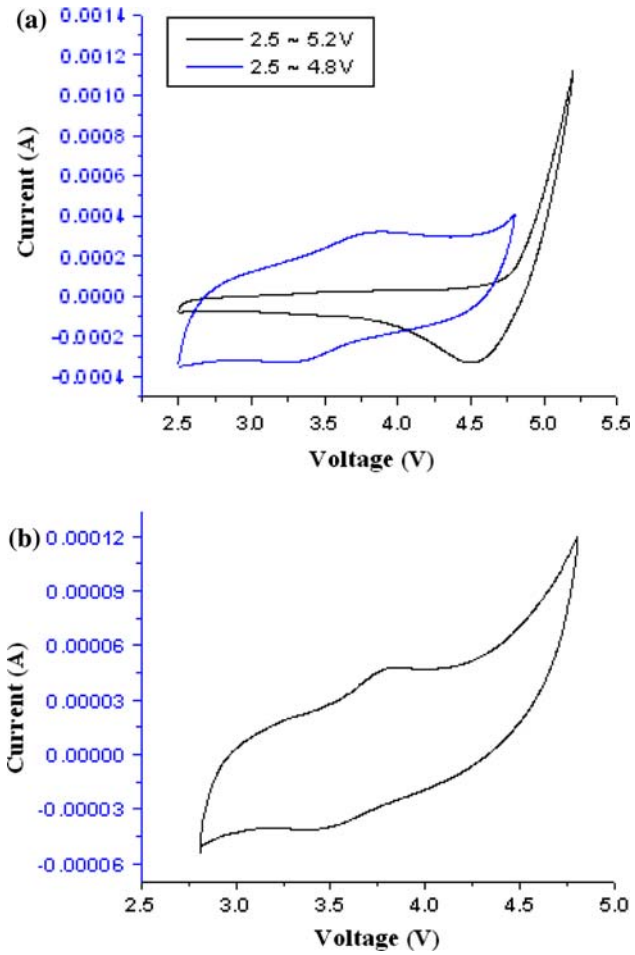

Fig. 7 Representative cyclic voltammogram of (**a**) $LiCoPO_4$ and (**b**) $LiNiPO_4$ cathodes sintered at 800 °C (5 h)

current rise is observed around 4.8 V, that may considered as the anodic peak along with a prominent cathodic peak at 4.5 V, which is in accordance with the reported results [21, 22].

Figure 7b shows the presence of an anodic peak at 3.82 V and a corresponding cathodic peak at 3.4 V due to $LiNiPO_4$ cathode cycled between 2.8 and 4.8 V. Generally it is reported that $LiNiPO_4$ prepared under air without the deployment of argon atmosphere and the addition of conducting carbon may not exhibit significant redox peaks, especially in the potential range 3.0–5.0 V [21, 23]. On the contrary, $LiNiPO_4$ synthesized using CAM sol–gel method and sintered in air through the present study has produced redox peaks at 3.8 and 3.5 V (Fig. 6b), which is noteworthy. Hence, it is claimed from the present study that CAM sol–gel method, especially due to the perfect tuning and monitoring of heating sequences along with the usage of select category gelling and chelating agents has resulted in the well formed cyclic voltamogram with the presence of the redox couple of Ni^{3+}/Ni^{2+} at the respective positions. Therefore, it is demonstrated from the study that the synthesis of $LiNiPO_4$ could be exempted from the requirement of stringent synthesis conditions that involves the deployment of argon atmosphere and carbon coating to the precursors mix provided suitable synthesis approach like CAM sol–gel method is followed. Because, it is believed that the CAM sol–gel method, by virtue of availability of excess of carbon would result in the in-situ addition of conducting carbon, thus exempting the need for stringent synthesis condition, which is the significance of select category CAM sol–gel method.

3.6.2 *Impedance measurements*

The EIS results of the as fabricated coin cells and cells after completing 25 CV cycles are displayed for $LiCoPO_4$ (Fig. 8a) and $LiNiPO_4$ (Fig. 8b). It is evident from Fig. 8a that the initial (R_1) as well as final internal resistance value (R_{25}) of the cell containing $LiCoPO_4$ cathode is found to differ by an insignificant value of 12 Ω only, i.e., such a small increase in internal resistance is negligible compared to the magnitude of initial (256 Ω) and final (268 Ω) impedance values of $LiCoPO_4$ cathode. Similarly, the difference in the internal resistance values of $LiNiPO_4$ cathode in the as fabricated ($R_1 = 65$ Ω) and in the cell after 25 cycles ($R_{25} = 73$ Ω) is also megar ($\Delta R = 8$ Ω), thereby substanting the fact that the CAM sol–gel synthesized $LiCoPO_4$ and $LiNiPO_4$ cathodes possess good storage as well as cycling stability, which is noteworthy. However, efforts to minimize the internal resistance of the cell upon cycling is underway. Further, it is understood from the study that the appreciable electro chemical behavior with a good structural stability of synthesized cathodes is

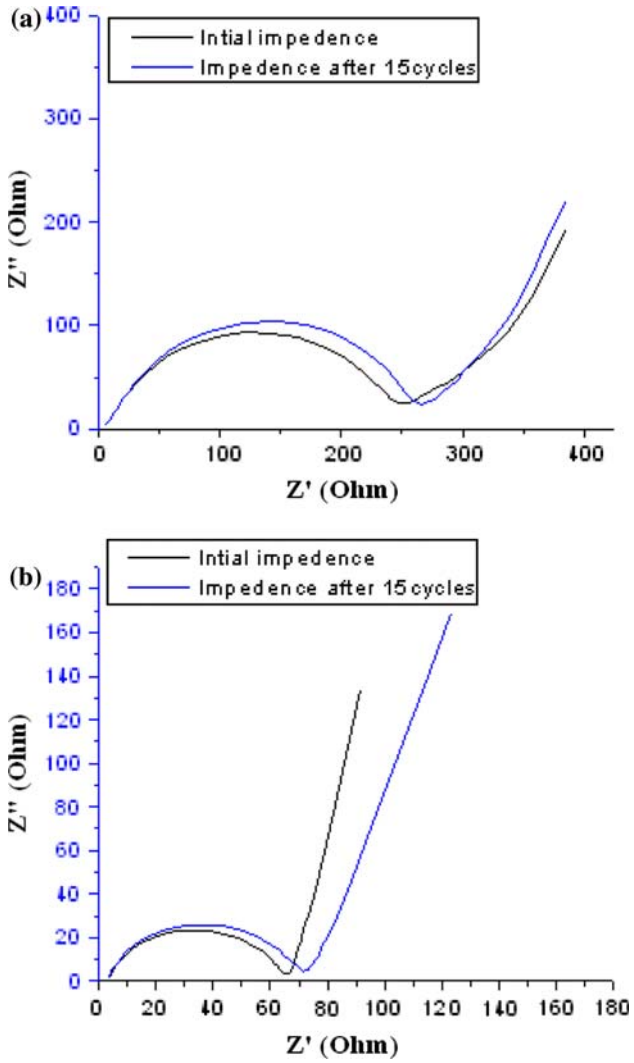

Fig. 8 **a** EIS behavior of $LiCoPO_4$ and **b** EIS behavior of $LiNiPO_4$

resulting from the synthesis methodology driven size reduced particles of phase pure $LiCoPO_4$ and $LiNiPO_4$ cathodes, which is highlight of the CAM sol–gel methodology.

4 Conclusions

$LiMPO_4$ (M=Co, Ni) category phospho-olivine cathode materials have been synthesized by adopting CAM sol–gel method. The chosen method is found to be advantageous in producing nanocrystalline $LiCoPO_4$ and $LiNiPO_4$ products with preferred physical and electrochemical properties required for rechargeable lithium-ion batteries. XRD results confirm the formation of above said compounds with an orthorhombic crystal lattice structure. TEM and FTIR results are in favor of nanometric particle size and preferred local cation environment, respectively. Further,

the cycleability and structural stability of the compounds are found to be excellent, thus recommended that $LiMPO_4$ (M=Co, Ni) cathodes could be considered as next generation lithium insertion electrode materials. Particularly, the possibility of synthesizing $LiNiPO_4$ at ambient synthesis conditions using CAM sol–gel method has been demonstrated through the study, thus excluding the reported category requirements of stringent synthesis conditions to prepare electrochemically active $LiNiPO_4$ cathode.

Acknowledgments The authors are thankful to the Council of Scientific and Industrial Research (CSIR), India for financial support to carry out this work.

References

1. Ni JF, Zhou HH, Chen JT, Zhang XX (2005) Mater Lett 59:2361–2365. doi:10.1016/j.matlet.2005.02.080
2. Nanjundaswamy KS, Padhi AK, Goodenough JB, Okada S, Ohtuka H (1996) Solid State Ion 92:1–10. doi:10.1016/S0167-2738(96)00472-9
3. Padhi AK, Nanjundaswamy KS, Goodenough JB (1997) J Electrochem Soc 144:1188–1194. doi:10.1149/1.1837571
4. Wang Y, Wang J, Yang J, Nuli Y (2006) Adv Funct Mater 16:2135–2141. doi:10.1002/adfm.200600442
5. Yamada A, Koizumi H, Sonoyama NN, Kanno R (2005) Electrochem Solid-State Lett 8(8):A409–A413. doi:10.1149/1.1945373
6. Revet N et al. (1999) Improved iron based cathode material. Abstract No.127. Electrochemical Society Fall meeting, Honululu, Hawaii
7. Huang H, Yin SC, Nazar LF (2001) Electrochem Solid-State Lett 4(10):A170–A172. doi:10.1149/1.1396695
8. Prosini PP, Zane D, Pasquali M (2001) Electrochim Acta 46:3517–3523
9. Chung SY, Blocking JT, Chiang YM (2002) Nat Mater 1:123–128. doi:10.1038/nmat732
10. Myung S-T, Komabo S, Hirosaki N, Yashiro H, Kumagai N (2004) Electrochem Acta 49:4213–4222
11. Jayaprakash N, Kalaiselvi N, Sun YK (2008) Electrochem Commun 13:455–460
12. Jayaprakash N, Kalaiselvi N, Periasamy P (2008) Nanotechnology 19:025603–025608. doi:10.1088/0957-4484/19/02/025603
13. Chen J, Vacchio MJ, Wang S, Chernova N, Zavalij PY, Wittingham MS (2008) Solid State Ion 178:1676–1693. doi:10.1016/j.ssi.2007.10.015
14. Jayaprakash N, Kalaiselvi N, Periasamy P (2008) Int J Electrochem Sci 3:478–488
15. Nakamoto K (1978) Infrared and Raman spectra of inorganic and coordination compounds. Wiley and sons, New York
16. Vivekanandan S, Venkateshwaralu M, Satyanarayana N (2008) Mater Chem Phys 109:241–248
17. Julien C, Camacho-Lopez MA, Mohan T, Chitra S, Kalyani P, Gopukumar S (2000) Solid State Ion 135:241–248. doi:10.1016/S0167-2738(00)00370-2
18. Rulmont A, Cahay R, Liegevis M, Tarte P (1991) Eur J Solid Inorg Chem 28:207–219
19. Ait salah A, Jozwiak P, Zaghib K, Garbarczyk J, Gendron F, Mauger A, Julien CM (2006) Spectrochem Acta A 65:1007–1013
20. Arcon D, Zorko A, Dominko R, Jaglicic Z (2004) J Phys Condens Matter 16:5531–5548. doi:10.1088/0953-8984/16/30/014
21. Okada S, Sawa S, Egashira M, Yamaki J, Tabuchi M, Kageyama H, Konishi T, Yoshino A (2001) J Power Sources 97–98:430–434. doi:10.1016/S0378-7753(01)00631-0
22. Amine K, Yasuda H, Yamachi M (2000) Electrochem Solid-State Lett 3(4):178–179. doi:10.1149/1.1390994
23. Wolfenstine J, Allen J (2005) J Power Sources 142:389–390. doi:10.1016/j.jpowsour.2004.11.024